

Accurate Channel Temperature Measurement in GaN-based HEMT Devices and its Impact on Accelerated Lifetime Predictive Models

B. Claflin^{a,b}, E. R. Heller^{a,b}, B. Winningham^c, J. E. Hoelscher^{a,b}, M. Bellott^c, K. Chabak^c,
A. Crespo^c, J. Gillespie^c, V. Miller^c, M. Trejo^c, G. H. Jessen^c, and G. D. Via^c

^a Materials and Manufacturing Directorate, AFRL/RXPS, WPAFB, OH 45433

^b Semiconductor Research Center, Wright State University, Dayton OH 45435

^c Air Force Research Laboratory, Sensors Directorate, Wright-Patterson AFB, Dayton, OH 45433

Phone: (937) 904-9937, email: bruce.claflin@wright.edu

Keywords: HEMT, infra-red thermal imaging, Raman, photoluminescence, thermography, electro-thermal modeling

ABSTRACT

Measurements of the channel temperature in a GaN-based HEMT device under DC bias are presented using IR thermal imaging, as well as μ -Raman and μ -PL spectroscopies for the *same* device. Comparison of the measured temperature values with simulated profiles from a full Sentaurus electro-thermal model can be used to validate the model and fine tune the materials-related simulation parameters. In addition, this comparison provides an estimate of the temperature error associated with each of these techniques and demonstrates the strengths and limitations of each method.

INTRODUCTION

Proper thermal management is critical for GaN-based HEMT devices because localized self-heating effects under high-power, high-frequency operation significantly impact device performance and reliability. Since heat generation is concentrated within a small volume at the drain-side edge of the gate contact [1], measurement of the temperature in the active region of the device requires high spatial resolution. For multi-finger devices, the boundary conditions are different for each channel resulting in a complex, non-uniform, 3-D temperature distribution across the device. Simple thermal models commonly used assume that heat is generated at the gate contact or from a limited region on the drain-side edge of the gate. More accurate, full electro-thermal models have been developed [1] to simulate the thermal profile of AlGaIn/GaN HEMT devices under operating conditions, and these device simulations can reproduce the I_d - V_d characteristics observed experimentally. However, time-to-failure predictions based on accelerated lifetime testing require accurate thermal profiles both at the point-of-failure and under normal operating conditions, because extrapolation of these data over several decades in time make the predictions extremely sensitive to small errors in temperature [2]. Several experimental probes are commonly used to measure temperature profiles of biased HEMT devices, such as IR thermal imaging [3], as well as μ -Raman [3-4] and μ -PL [5] spectroscopies. Each of these techniques has its own unique advantages and disadvantages for this purpose, and they each provide limited spatial information. In this work, InAl(Ga)N/GaN HEMT channel

temperature profiles are measured using IR thermal imaging, μ -Raman mapping, and μ -PL mapping in the *same* device under identical DC bias conditions, to allow direct comparison of the results from each technique. These temperature measurements are also compared with a full electro-thermal model simulation of the operating device to evaluate and understand the limitations of each technique.

EXPERIMENTAL

The device studied was a 2x150 μm wide, 0.25 μm long InAl(Ga)N/GaN HEMT with 3 μm source/drain spacing and the following epilayer structure: 10 nm of InAl(Ga)N with a 1 nm AlN interlayer on a 50 nm GaN channel, a 1.5 μm AlGaIn buffer (4% Al) and a 100 nm AlN nucleation layer on a thinned Si substrate. Thermal maps were recorded using a QFI Infrascopes III IR thermal imager and using a custom-built μ -Raman/ μ -PL apparatus with bias conditions of $V_{ds}=10$ V and $I_{ds}=184$ mA (1.84 W total dissipated power) in an ACCEL-RF DUT module. The device was operated with the heated baseplate set to 85 $^{\circ}\text{C}$ to provide a uniform thermal background for IR imaging. The same baseplate heating conditions were used for both μ -Raman and μ -PL mapping for consistency and to allow direct comparison of the results. The 514 nm Ar^+ laser line was used as the excitation source for confocal μ -Raman measurements in backscattering geometry. A 100x objective lens was used to focus the laser to ~ 1 μm diameter spot and to collect the scattered light. Since the 514 nm line is below the bandgap of GaN, no absorption occurs or laser-induced heating during μ -Raman measurements. The accuracy of the μ -Raman temperature measurements is ~ 10 $^{\circ}\text{C}$ [6]. Confocal μ -PL measurements in backscattering geometry were made using 325 nm HeCd laser excitation. A 39x UV objective focused the laser to ~ 3 μm diameter spot and collected the resulting luminescence. Since the absorption coefficient of GaN is $\sim 1.2 \times 10^5$ cm^{-1} at 325 nm [7], the absorption depth of the laser is only ~ 0.25 μm . Neutral density filters were used to reduce the power on-sample to minimize laser-induced heating. The accuracy of temperatures determined by μ -PL is ~ 10 $^{\circ}\text{C}$ [5]. Both μ -Raman and μ -PL spectra were measured with a thermo-electrically cooled Si CCD detector

and a $\frac{1}{2}$ m spectrometer. High resolution μ -Raman and μ -PL maps were recorded using a computer controlled X-Y stage with 1 μ m steps. Measurements of the temperature shifts of the GaN $E_2(\text{high})$ and SiC $E_2(\text{TO})$ phonon modes (Raman) as well as the temperature shift of the GaN near-band-edge PL peak wavelength were performed up to 250 $^{\circ}\text{C}$ on the unpowered device for calibration purposes by heating the baseplate and allowing the temperature to stabilize. A 3-D finite element thermal model was constructed for this device in ANSYS [8]. The thermal diffusion equation is solved for a 500 μm x 500 μm x 100 μm thick SiC substrate bonded to a brass baseplate maintained at 85 $^{\circ}\text{C}$ by a 35 μm thick layer of EPO-TEK H20E-HC thermal epoxy. Adiabatic boundary conditions are used everywhere except for the bottom of the baseplate (isothermal boundary conditions). The two gate fingers are centered on the die and assumed to generate heat uniformly along their entire width. Active device epilayers are modeled electro-thermally using Sentaurus Device [9], with the coupled solution of the drift-diffusion equations (Poisson equation and the electron continuity equations) and the thermal diffusivity equation. As before, the device boundary conditions at the top and sides are adiabatic, but the bottom is linked to the thermal simulation [1]. Joule heating is incorporated into the model from the solution of the drift-diffusion equations throughout the channel. Most of the resulting heat is concentrated near the gate as expected.

RESULTS AND DISCUSSION

A common technique for temperature measurement in GaN-based HEMT devices is IR thermal imaging as seen in Fig. 1. This method is fast, convenient, and non-destructive. However, this approach does not provide the spatial resolution needed for failure prediction of high-performance devices because of its 3-5 μm diffraction-limited spatial resolution. Difficulties with emissivity calibration of the device structure result in underestimation of the operating temperature. For the device shown in Fig. 1, the measured peak channel temperature is ~ 185 $^{\circ}\text{C}$, while far from the active device region a temperature of ~ 107 $^{\circ}\text{C}$ is recorded.

When the same device is measured under identical operating conditions using μ -Raman mapping, (Fig. 2), the peak channel temperature is found to be ~ 225 $^{\circ}\text{C}$. Far from the active region of the device, the measured temperature is ~ 140 $^{\circ}\text{C}$. Determination of these value relies on the (measured) temperature dependence of the GaN $E_2(\text{high})$ phonon frequency, shown in Fig. 3, which agrees with previously reported values [6]. Since GaN is transparent to the Raman excitation laser, it is possible to simultaneously map the thermal profile in the SiC substrate (Fig. 4) using the temperature dependence of the SiC $E_2(\text{TO})$ phonon frequency (Fig. 5). The peak temperature measured in the SiC substrate, under the channel, is ~ 140 $^{\circ}\text{C}$, which is substantially lower than the value measured near the gate, in the GaN layer. Far from the active region of the device, the temperature measured in the SiC substrate is ~ 125 $^{\circ}\text{C}$. One

of the limitations of the Raman method of thermography is its finite depth resolution which typically extends ~ 2 -4 μm

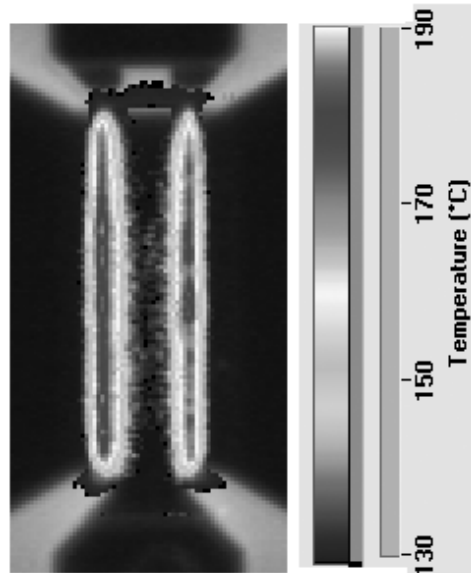


Fig. 1 IR thermal image of an AlIn(Ga)N/GaN HEMT device operated under DC bias of $V_d=10$ V and $I_d=184$ mA.

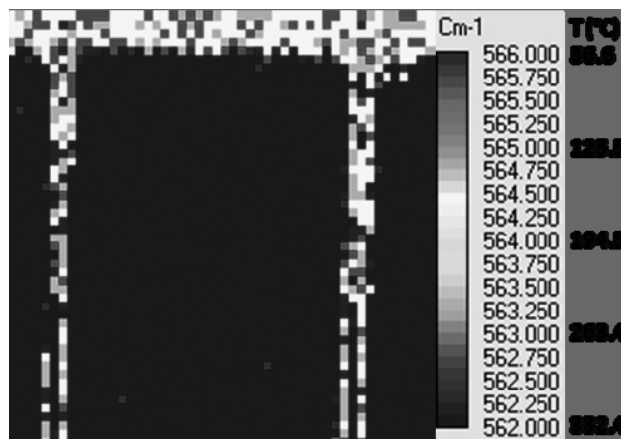


Fig. 2 Temperature map of the same HEMT device as Fig. 1 under identical operating conditions, derived from the shift of the GaN $E_2(\text{high})$ phonon frequency measured by μ -Raman.

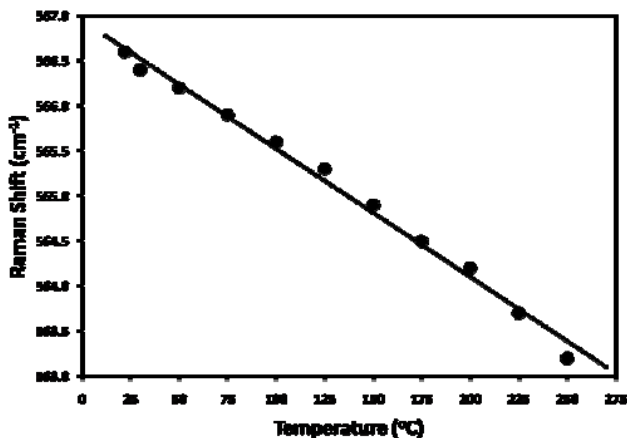


Fig. 3 Temperature shift of the GaN E₂(high) phonon frequency measured by μ -Raman.

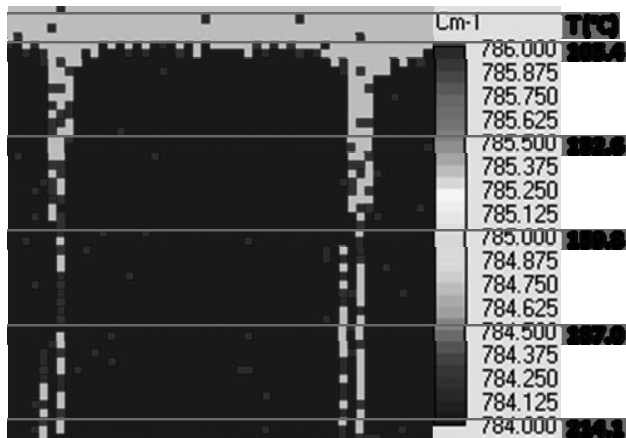


Fig. 4 Simultaneous SiC thermal profile derived from the shift of the E₂(TO) phonon frequency measured by μ -Raman.

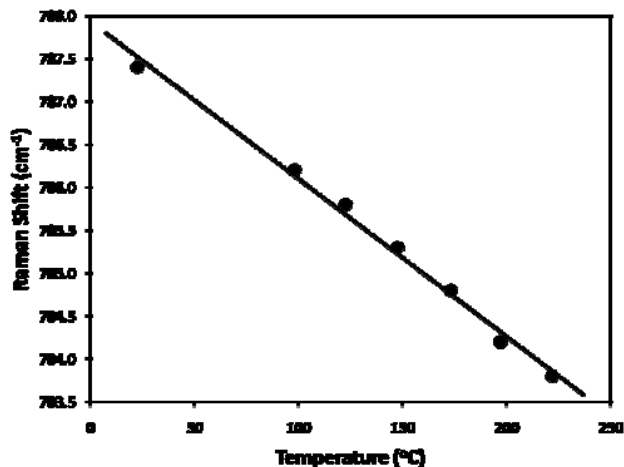


Fig. 5 Temperature shift of the SiC E₂(TO) phonon frequency measured by μ -Raman.

for a system utilizing a confocal microscope [6]. Usually, the active GaN layer is thinner than this depth, so the Raman measurement gives an average temperature from the entire

layer. As the measurements from the GaN and SiC layers (above) have demonstrated, there can be a substantial thermal gradient in the vertical direction, so the Raman technique may also slightly underestimate the peak operating device temperature, although not by as much as the IR thermal imaging method. In addition, because of the lower signal to noise ratios inherent in the Raman scattering process, longer integration times are required than for the other techniques, resulting in lower sample throughput.

When the same HEMT device shown in Figs. 1 and 2 is measured under identical operating conditions using μ -PL mapping, (Fig. 6), the peak channel temperature close to the gate is found to be ~ 238 °C. Far from the active region of the device, the measured temperature is ~ 140 °C. These values rely on the temperature dependence of the GaN near-band-edge PL peak wavelength, shown in Fig. 7, which agrees with previously reported values [5, 10]. Since the

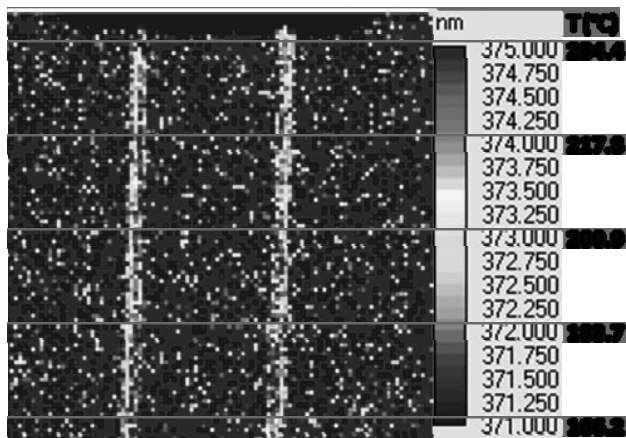


Fig. 6 Temperature map of the same HEMT device as Figs. 1 and 2 under identical operating conditions, derived from the shift of the GaN near-band-edge PL peak wavelength.

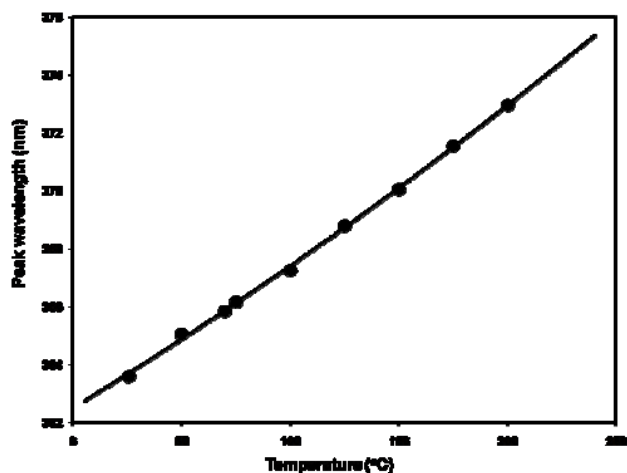


Fig. 7 Temperature shift of the GaN near-band-edge PL peak wavelength.

absorption depth of the 325 nm laser is only ~ 0.25 μm , PL is an attractive, high resolution method to probe the drain side edge of the gate where the temperature is highest. However,

the use of PL for thermography in GaN-based HEMT devices also has several significant limitations. Because PL relies on photon absorption, laser-induced heating is a major concern and the on-sample laser power should be minimized to ensure accurate temperature measurement. Also, the laser excitation generates electron-hole pairs which can modify the depletion layer in the channel, resulting in photo-induced drain current [11]. In the most extreme case, photo-excitation can degrade the HEMT device performance and cause premature failure.

Electro-thermal model simulations are shown in Fig. 8 for the InAl(Ga)N/GaN HEMT device operating under the same conditions used experimentally. Far from the active region of the device, the model predicts $T \sim 120^\circ\text{C}$ in the SiC substrate and the epilayers, with only a 2-3 $^\circ\text{C}$ drop across the entire SiC die thickness. This agrees well with the SiC temperature measured by Raman but is slightly lower than

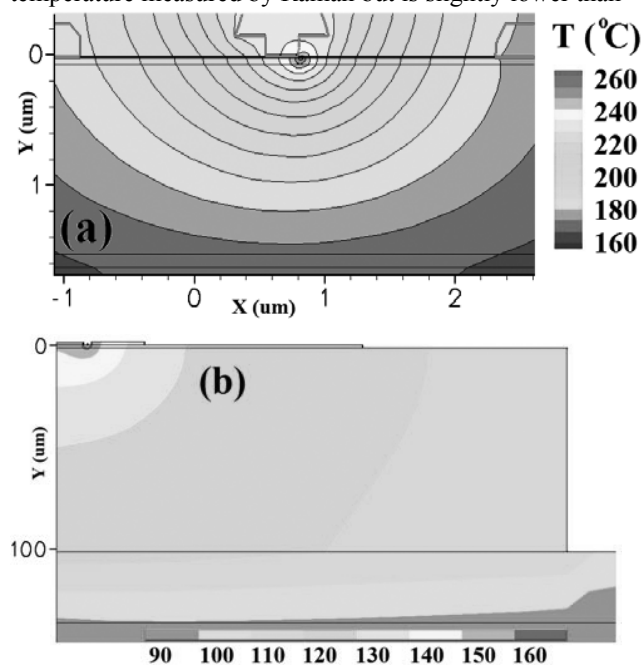


Fig. 8 Electro-thermal model simulated temperature profile in the epilayers (a) and in the SiC die (b) at the 184mA, 10V bias point. Both (a) and (b) show a cut through the center of the gate. Due to symmetry, only half of the device and one finger is shown in (b).

the epilayer temperatures determined by both Raman and PL, and is slightly higher than the temperature measured by IR thermal imaging. Comparisons of channel temperatures between the model and experimentally measured values is more difficult, because the temperature varies rapidly with position over the length scales probed by the three different techniques as seen in Fig. 8 (a). The simulated peak temperature is 255°C at the InAl(Ga)N/GaN interface under the T-gate, but only $\sim 225^\circ\text{C}$ at the hottest point that is optically accessible based on line-of-sight, $\sim 0.3\ \mu\text{m}$ from the drain-side edge of the gate. This temperature agrees quite well with those measured by Raman and PL, but IR thermal

imaging underestimates this peak channel temperature by $\sim 40^\circ\text{C}$. At the SiC/AlGaIn interface, directly below the drain-side edge of the gate, the simulated temperature is $\sim 172^\circ\text{C}$, resulting in a vertical thermal gradient of $\sim 83^\circ\text{C}$. This value closely matches the $\sim 85^\circ\text{C}$ vertical gradient derived from Raman measurements in the GaN and SiC layers, although in the optically accessible region, the simulated value drops by $\sim 53^\circ\text{C}$ which is somewhat less than the measured value. Given the uncertainties in the Raman measurements, this difference seems reasonable. At the bottom of the SiC die, directly below the drain-side edge of the gate, the model temperature drops to 128°C . This $\sim 44^\circ\text{C}$ thermal gradient across the SiC substrate contrasts with points far from the active region of the device which exhibit almost no thermal gradient as shown above. Again, this difference is reasonable given the much greater heat flux near the gate.

CONCLUSIONS

Temperature profiles were measured on the same operating InAl(Ga)N/GaN HEMT device using IR thermal imaging, μ -Raman and μ -PL spectroscopies. Both μ -Raman and μ -PL gave comparable peak temperatures in the device channel and far from the active region, while for both regions IR thermal imaging underestimated the temperature by 30-40 $^\circ\text{C}$. A vertical thermal gradient of $\sim 85^\circ\text{C}$ was seen between the GaN epilayer and the SiC substrate with μ -Raman. Device simulations using a full Sentaurus electro-thermal model give good agreement for the channel temperatures determined from Raman and PL measurements as well as the thermal gradient between the InAl(Ga)N/GaN interface and the SiC substrate directly below the gate.

ACKNOWLEDGEMENTS

The work of BC, ERH, and JEH was supported by AFRL Contract #FA8650-06-D-5401 and AFOSR (D. Silversmith).

REFERENCES

- [1] E. R. Heller and A. Crespo, *Microelectron. Reliab.* **48**, 45 (2008).
- [2] E. R. Heller, *IEEE Transactions on Electron Devices* **55**, 2554 (2008).
- [3] A. Sarua, H. Ji, M. Kuball, M. J. Uren, T. Martin, K. P. Hilton, and R. S. Balmer, *IEEE Trans. Electron Devices* **53**, 2438 (2006).
- [4] M. Kuball, J. M. Hayes, M. J. Uren, T. Martin, J. C. H. Birbeck, R. S. Balmer, and B. T. Hughes, *IEEE Electron Device Lett.* **23**, 7 (2002).
- [5] N. Shigekawa, K. Onodera, and K. Shiojima, *Jpn. J. Appl. Phys.* **42**, 2245 (2003).
- [6] M. Kuball, J. W. Pomeroy, S. Rajasingam, A. Sarua, M. J. Uren, T. Martin, A. Lell, and V. Härle, *Phys. Stat. Sol. A* **202**, 824 (2005).
- [7] J. F. Muth, J. D. Brown, M. A. L. Johnson, Z. Yu, R. M. Kolbas, J. W. Cook, JR, and J. F. Schetzina, *MRS Internet J. Nitride Semicond. Res.* **4S1**, G5.2 (1999).
- [8] *ANSYS/Mechanical Software Suite*, ANSYS, Inc., Canonsburg, PA.
- [9] Synopsys, Inc, Mountain View, California, Sentaurus Device User Manual, Version A-2007.12, 2007.
- [10] A. P. Young and L. J. Brillson, *Appl. Phys. Lett.* **77**, 699 (2000).
- [11] T. Mizutani, *Jpn. J. Appl. Phys.* **21**, L479 (1982).

Acronyms

- HEMT: High-electron-mobility transistor
- DC: direct current
- IR: infra-red
- μ -PL: micro-photoluminescence
- I_d : drain current
- V_d : drain voltage